Bull Volcanol (1998) 60:110–124

ORIGINAL PAPER

C. F. Waythomas · C. A. Neal

Tsunami generation by pyroclastic flow during the 3500-year B.P. caldera-forming eruption of Aniakchak Volcano, Alaska

Received: 3 December 1997 / Accepted: 11 April 1998

Abstract A discontinuous pumiceous sand, a few centimeters to tens of centimeters thick, is located up to 15 m above mean high tide within Holocene peat along the northern Bristol Bay coastline of Alaska. The bed consists of fine-to-coarse, poorly to moderately well-sorted, pumice-bearing sand near the top of a 2-m-thick peat sequence. The sand bed contains rip-up clasts of peat and tephra and is unique in the peat sequence. Major element compositions of juvenile glass from the deposit and radiocarbon dating of enclosing peat support correlation of the pumiceous sand with the caldera-forming eruption of Aniakchak Volcano. The distribution of the sand and its sedimentary characteristics are consistent with emplacement by tsunami. The pumiceous sand most likely represents redeposition by tsunami of climactic fallout tephra and beach sand during the approximately 3.5 ka Aniakchak caldera-forming eruption on the Alaska Peninsula. We propose that a tsunami was generated by the sudden entrance of a rapidly moving, voluminous pyroclastic flow from Aniakchak into Bristol Bay. A seismic trigger for the tsunami is unlikely, because tectonic structures suitable for tsunami generation are present only south of the Alaska Peninsula. The pumiceous sand in coastal peat of northern Bristol Bay is the first documented geologic evidence of a tsunami initiated by a volcanic eruption in Alaska.

Key words Tsunami deposit · Pyroclastic flow · Aniakchak caldera · Volcanigenic tsunami

Introduction

Volcanic eruptions often result in the rapid transfer of mass from areas high on the volcano flank to lower areas on or adjacent to the volcano. For volcanoes situated on or near the coastline, rapid mass transfer may cause impulse-generated water waves or volcanigenic tsunami (Latter 1981; Self and Rampino 1981; Nomanbhoy and Satake 1995). In the Aleutian volcanic arc more than 40 active volcanoes are located a few tens of kilometers or less from the coastline (Fig. 1). At many of these eruptive centers, exposures in nearby coastal sea bluffs show pyroclastic flows, lahars, and debris avalanches that flowed into the sea. Future eruptions of Aleutian arc volcanoes could generate tsunamis if associated with large-scale flank collapses, or if debris avalanches or pyroclastic flows enter the sea rapidly.

Hazards from volcanigenic tsunami in the Cook Inlet region of southern Alaska have been discussed for Augustine (Kienle et al. 1987; Begét and Kienle 1992; Siebert et al. 1995; Troshina 1996; Waythomas 1997) and Redoubt volcanoes (Waythomas et al. 1998), but the topic of tsunami generation by caldera-forming eruptions in Alaska has received limited attention (Waythomas et al. 1995). Eight or more caldera-forming eruptions with volumes of 10 km^3 or more (bulk volume) have occurred in the Holocene, and pyroclastic-flow deposits from most Holocene volcanic centers extend to the present coastline (Miller and Smith 1987). One such example is Aniakchak Volcano, a young, well-exposed, and historically active caldera, currently being studied by workers of the Alaska Volcano Observatory (Neal et al. 1995). This paper presents sedimentologic and other evidence for a tsunami associated closely in time with the caldera-forming eruption that occurred ~3500 years B.P.

Formation of Aniakchak caldera

Aniakchak caldera is a 10-km-diameter, 0.5-to-1.0-km-deep, circular caldera located within Aniakchak National Monument and Preserve, approximately 670 km southwest of Anchorage on the Alaska Peninsula

Editorial responsibility: D. Swanson

C. F. Waythomas (✉) · C. A. Neal
U.S. Geological Survey, Alaska Volcano Observatory,
4230 University Drive, Anchorage, Alaska 99508, USA

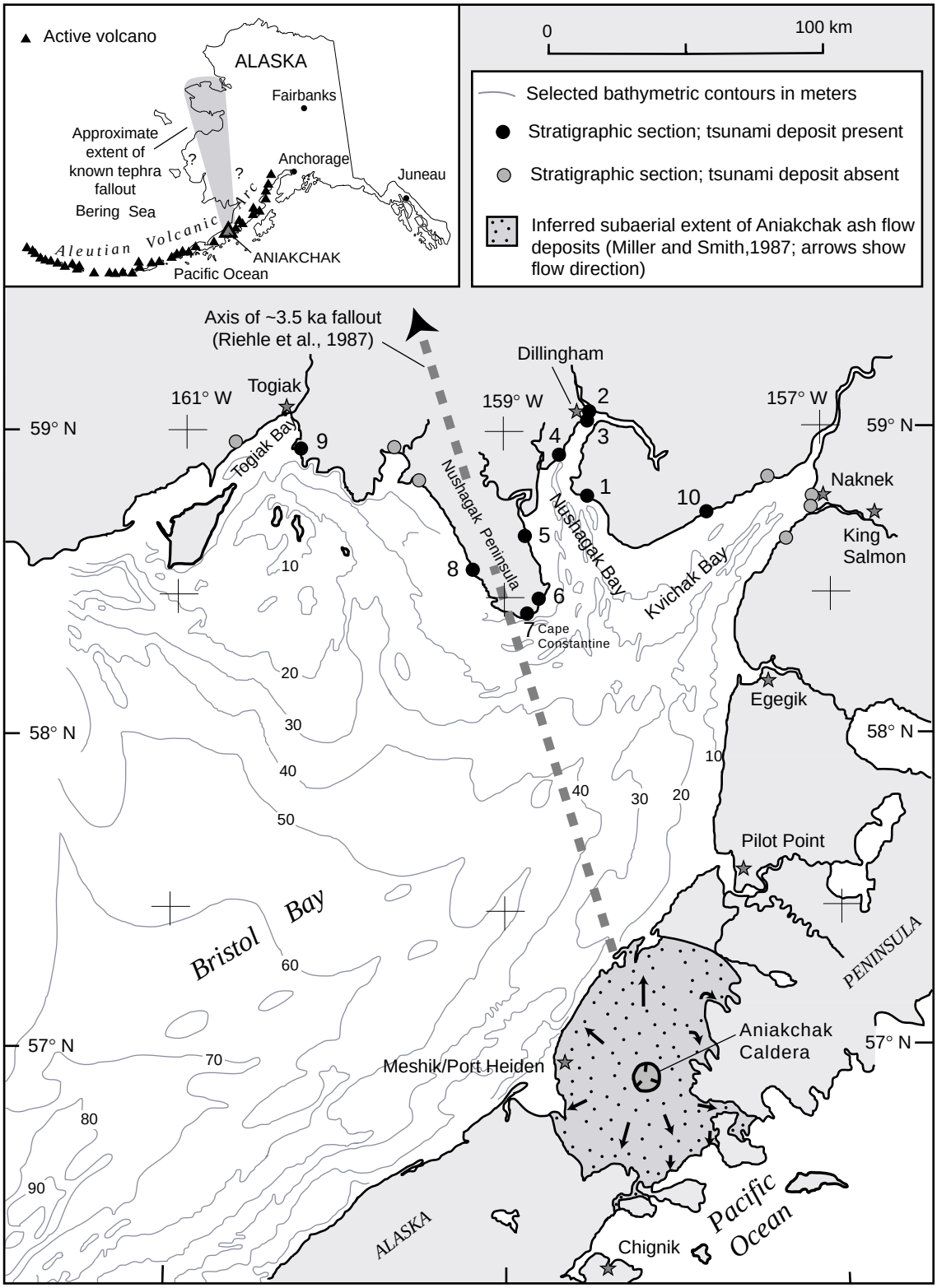

Fig. 1 Upper Bristol Bay, showing location of stratigraphic sections, Aniakchak caldera and extent of ash-flow sheet, and axis of tephra fallout from the ~3500-year B.P. eruption. Bathymetric data from the National Oceanic and Atmospheric Administration, Naknek, Hagemeister Island, Ugashik and Sutwik Island sheets 1988, 1:250000 scale. Extent of tephra plume from Begét et al. (1992)

(Fig. 1). The caldera was formed during a catastrophic eruption that obliterated a pre-existing andesitic stratocone, distributed volcanic ash northward into arctic Alaska (Riehle et al. 1987; Begét et al. 1992), and generated an extensive ash-flow sheet (Miller and Smith 1977). The timing of this eruption is well constrained by

radiocarbon dating of fallout and pyroclastic-flow deposits at ~3500 years B.P. (Miller and Smith 1977; Riehle et al. 1987; Begét et al. 1992). Magmatic activity has continued within the caldera, and the most recent eruption was in 1931 (Neal et al. 1995).

The climactic Aniakchak eruption was accompanied by voluminous tephra fall from plinian columns that probably extended >20 km above sea level. The generalized distribution of tephra fallout from the caldera-forming eruption determined by Riehle et al. (1987) and Begét et al. (1992) defines a single, narrow sector with an axis extending approximately north–northwestward from the caldera (Fig. 1). During the eruption, most of upper Bristol Bay received considerable coarse lapilli fallout.

Pyroclastic-flow deposits from the caldera-forming eruption extend to both the Pacific and Bering Sea coasts, southeast and northeast of the caldera, respectively (Fig. 1). From this distribution, Miller and Smith (1987) inferred the original extent of the pyroclastic-flow deposits, which are now largely buried by post-caldera tephra and other surficial deposits (Fig. 1). The Aniakchak pyroclastic-flow deposits are mostly unconsolidated, rich in coarse pumice and scoria, and compositionally zoned (Miller and Smith 1977). Welded units are a small proportion of the deposit. A maximum thickness of more than 100 m is estimated where pyroclastic flows have ponded against the relief of the Aleutian Range (Miller and Smith 1977). In coastal bluffs along the Bristol Bay shoreline, the pyroclastic-flow deposits are at least 15 m thick and consist of a single massive bed. The volume of material erupted during caldera formation was >50 km^3 (Miller and Smith 1987), and as much as 75% of this volume was pyroclastic-flow deposits. Evidence for extreme mobility (and hence, high velocity) of this pyroclastic flow during emplacement includes its transit over several-hundred-meter-high mountain passes in the Aleutian Range and across narrow bays on the Pacific Coast (Miller and Smith 1977; T.P. Miller, pers. commun.).

We hypothesize that a large tsunami was initiated during the caldera-forming eruption as the extensive pyroclastic-flow sheet rapidly entered the southern Bering Sea. Herein we describe a pumiceous sand deposit discovered during investigations of the upper Bristol Bay coastline by Lea (1989) that records widespread tsunami inundation of the Nushagak Peninsula and other areas near Dillingham, Alaska (Fig. 1).

Field characteristics of the pumiceous sand

Lea (1989) and Allen (1994) were the first to report a discontinuous, pumice-bearing sand within Holocene peat deposits along the Nushagak Peninsula on the north shore of Bristol Bay (Fig. 1). Based on radiocarbon dating and the unique stratigraphic character of the pumiceous sand, both Lea (1989) and Allen (1994) suggested an origin by seismogenic tsunami possibly associated with the Aniakchak caldera-forming eruption. To further investigate the significance of the pumiceous sand as part of hazard investigations related to Aniakchak caldera, we examined numerous coastal-bluff sites from Kvichak Bay westward to Togiak Bay (Figs. 1, 2).

The pumiceous sand is a discontinuous, poorly to moderately well-sorted, light-gray to orange-tan, fine-to-coarse sand bed as thick as 40 cm (Figs. 2, 3). The deposit is not obviously reworked, but it tends to be thicker at higher elevations, where it may have been partially reworked by backwash and return flow. Sedimentary structures associated with bidirectional currents were not observed, and in only a few places does the deposit exhibit faint lamination. In most places along the Nushagak Peninsula, it is near the top of a 1- to 4-m-thick uniform sequence of woody peat that overlies Pleistocene glacial deposits (Lea 1989, 1990; Lea et al. 1991). The height of the pumiceous sand above mean high tide as measured by hand level ranges from 1 to 15 m. Where thickest, the pumiceous sand is massive, and faint bedding or thin lenses of varying grain size and color are present in some places. Rip-up clasts of peat, some up to 20 cm long, also occur in the deposit. The pumiceous sand fills irregularities in the underlying peat, giving rise to pinch and swell variations in thickness over distances of a few tens of meters in the outcrop face. At some locations the pumiceous sand is preserved as a single conspicuous lens or stringer of coarse sand in the woody peat. The lenses themselves may contain disseminated fragments of peat.

At two locations (sites 3 and 5, Fig. 1) a thin (<1 cm), light gray to gray-orange, fine-ash deposit (hereafter called the basal ash) is present at the base of the pumiceous sand (Allen 1994). The ash varies from a continuous, distinct layer mantling the hummocky peat surface to discontinuous pockets or thin "smears" of ash. Rounded pods of reworked fine basal ash up to 5 cm across also are present in the main pumiceous sand unit. The basal ash likely represents an early phase of tephra fallout prior to the climactic eruption.

The pumiceous sand consists of subangular to moderately well-rounded, buff to light brown or mixed color, frothy, glassy, pumice; crystal fragments (primarily feldspar, pyroxene, and hornblende); both clear and dark vitric shards; and <10% detrital grains. At the tip of the Nushagak Peninsula (site 7, Fig. 1) where the pumiceous sand is coarsest, the maximum pumice clast size is approximately 1 cm, similar to that reported by Lea (1989).

Distribution

The pumiceous sand crops out from the eastern shoreline of Nushagak Bay westward as far as the southeast entrance of Togiak Bay (Fig. 1). Southwest of Togiak, it is conspicuously absent in low bluffs that lack peat or where the peat is poorly developed. Wet, poorly

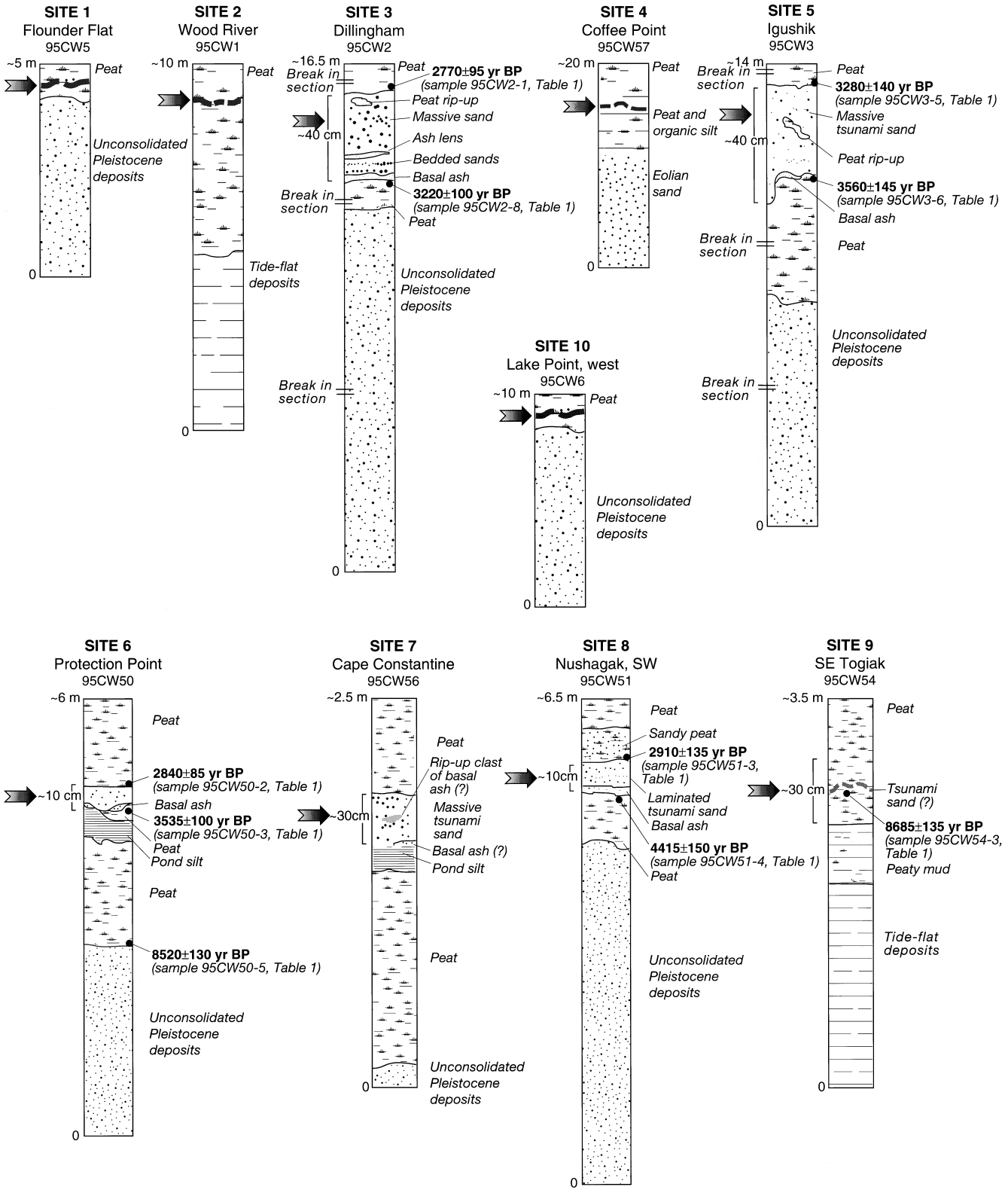

Fig. 2 Stratigraphic profiles from upper Bristol Bay coastline. *Arrows* show position of pumiceous sand. Base of each section is approximately mean high tide. Location of sites given in Fig. 1

drained areas favoring peat development apparently were the best sites for rapid burial and preservation of the pumiceous sand. Lea (1989) reported pumiceous sand in upper Kvichak Bay, but we recognized the pumiceous sand at only one location in this area, even though bluffs with thick deposits of capping peat are

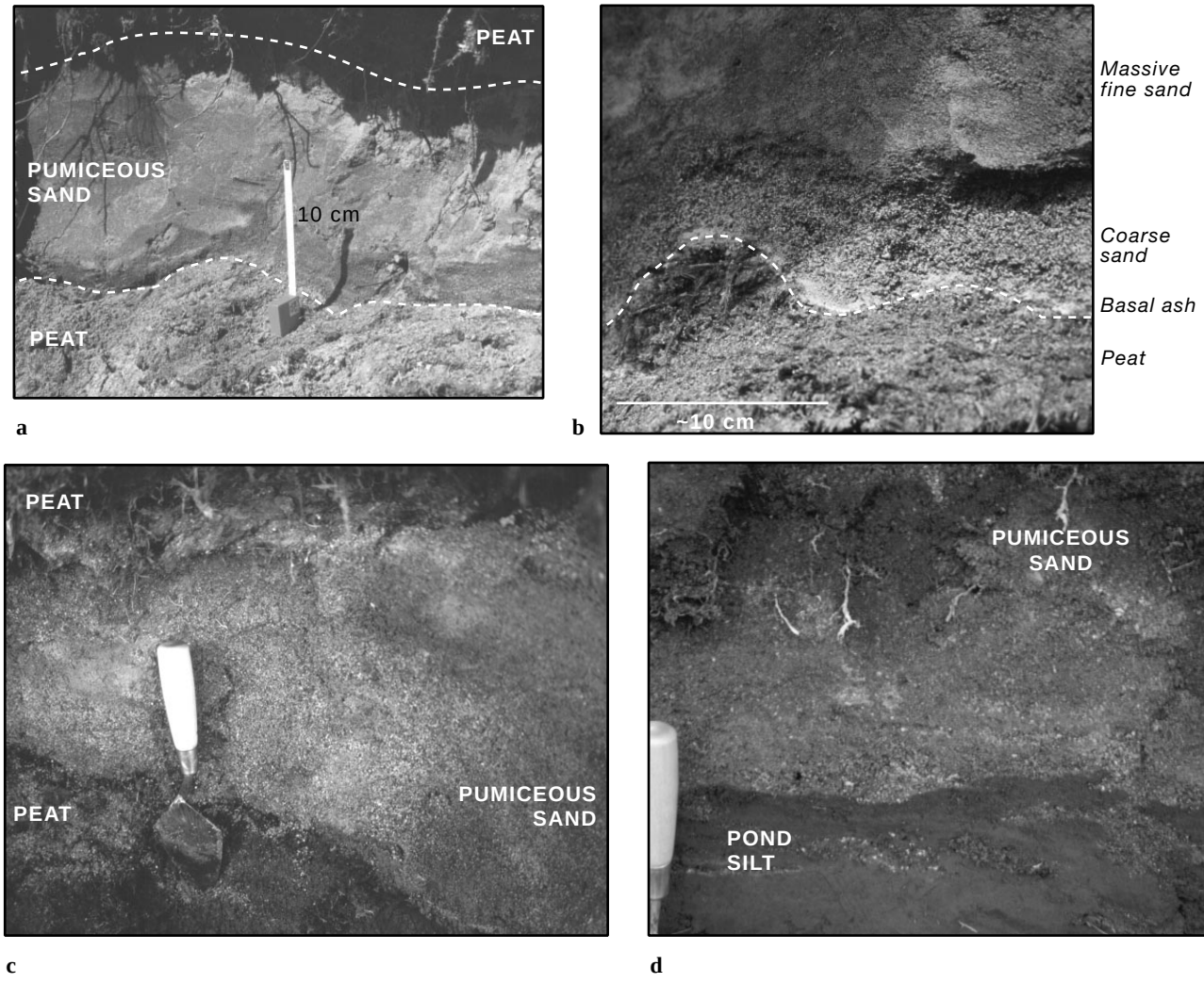

Fig. 3a–d Representative photographs of the pumiceous sand. **a** Site 3 at Dillingham; **b** closeup of basal part of section at site 3; **c** site 5, Igushik; **d** site 7, Cape Constantine. Length of trowel handle in photographs c and d is about 10 cm

common. We have not dug pits through the peat inland from the coastal bluffs to determine the landward characteristics of the deposit.

Radiocarbon dating

Radiocarbon ages of peat from deposits just below the pumiceous sand support deposition coincident with the Aniakchak eruption (Fig. 4; Table 1). The mean weighted radiocarbon age (Stuiver and Reimer 1993) of 11 samples of soil-organic matter and charcoal immediately below or in Aniakchak fallout tephra or ash-flow deposits is 3551 ± 30 years B.P. The mean weighted radiocarbon age of five peat samples collected from the contact zone at the base of the pumiceous sand is 3547 ± 50 years B.P. One age (95CW54–3: 8685 ± 135 years B.P.; Table 1) falls well outside this range associated with the caldera-forming eruption. This sample was collected from beneath a thin, discontinuous lens of medium-to-coarse, slightly pumiceous sand (site 9, Fig. 2) that, because of its age, we do not correlate with the 3500-year-old pumiceous sand; however, it may be an older tsunami deposit.

A radiocarbon age of 8520 ± 130 (calibrated age ca. 9500 years B.P.; Table 1) from the base of a peat section at site 6 (Protection Point; Figs. 1, 2) dates the onset of peat accumulation on the Nushagak Peninsula. No other deposits like the pumiceous sand have been found in peat deposits in the upper Bristol Bay area, with the exception of the sand bed near Togiak (site 9, Figs. 1, 2). Thus, the stratigraphic data and radiocarbon dates indicate that the pumiceous sand is a unique component of the Holocene stratigraphic record in upper Bristol Bay.

Geochemical evidence of sand source

Major element compositions of juvenile glass from both the pumiceous sand and the basal ash correlate well with compositions of glass separates from proximal and distal climatic Aniakchak fallout and pyroclastic-flow

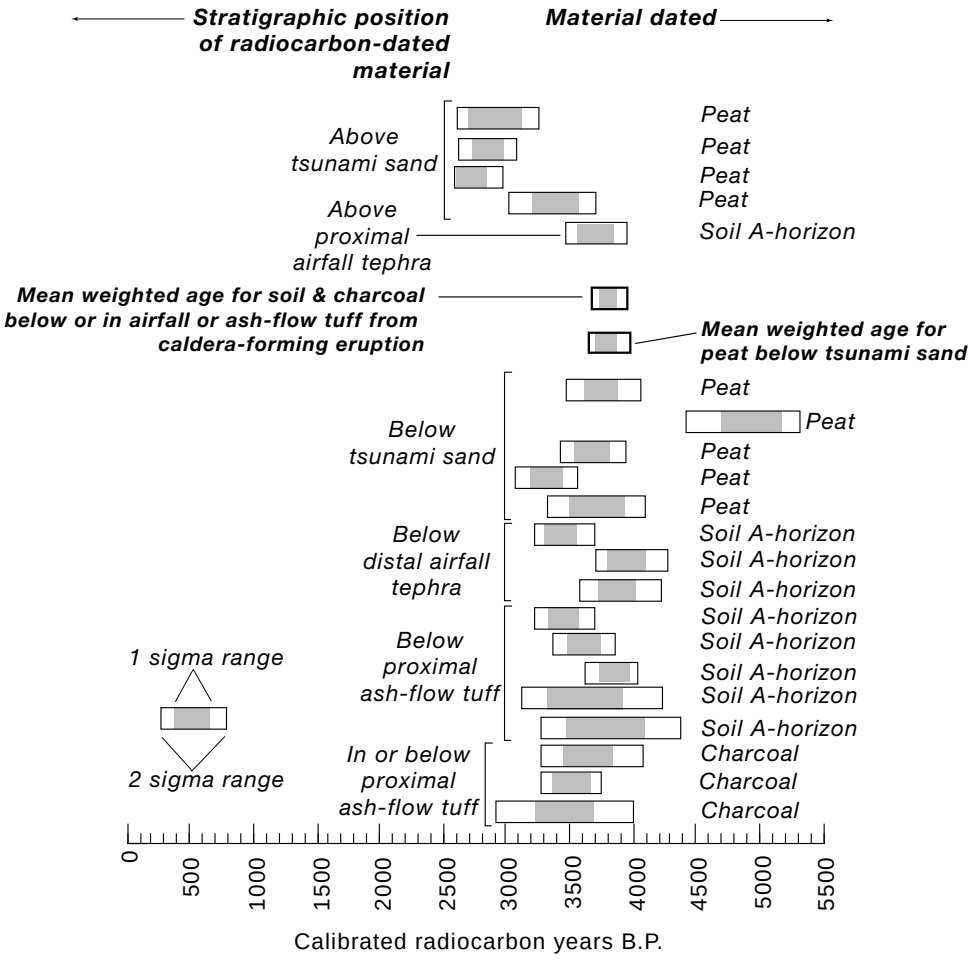

Fig. 4 Summary of radiocarbon ages related to deposits associated with the ~3500-year B.P. caldera-forming eruption of Aniakchak Volcano. Data from Riehle et al. (1987), Miller and Smith (1987), Begét et al. (1992), and this study. All dates calibrated by method of Stuiver and Reimer (1993)

Table 1 Radiocarbon dates from coastal sections in upper Bristol Bay [Dates calibrated using method of Stuiver and Reimer (1993), reported as -1σ **age** $+1\sigma$; BP ages reported with respect to year AD 1950; all material dated is peat]

Location and sample no.	Lab. no.	Reported age (C-14 years BP)	$\delta^{13}C_{PDB}$	Calibrated age (years BP)	Sample collection notes and location
Site 5 95CW3-5	GC-21324	3280 ± 140	−28.2	3684, **3471**, 3359	Contact zone above tsunami deposit; Igushik section
Site 5 95CW3-6	GX-21325	3560 ± 145	−27.2	4074, **3836**, 3537	Contact zone below tsunami deposit; Igushik section
Site 3 95CW2-1	GX-21371	2770 ± 95	−27.5	2957, **2855**, 2765	Contact zone above tsunami deposit; Dillingham section
Site 3 95CW2-8	GX-21323	3220 ± 100	−22.3	3556, **3453, 3426, 3411,** 3350	Contact zone below tsunami deposit; Dillingham section
Site 6 95CW50-2	GX-21372	2840 ± 85	−28.1	3068, **2943,** 2849	Contact zone above tsunami deposit; Protection Point section
Site 6 95CW50-3	GX-21373	3535 ± 100	−27.3	3925, **2829, 3780, 3778,** 3657	Contact zone below tsunami deposit; Protection Point section
Site 6 95CW50-5	GX-21374	8520 ± 130	−29.0	9537, **9484,** 9388	Base of peat section; indicates beginning of peat accumulation; Protection Point section
Site 8 95CW51-3	GX-21375	2910 ± 135	−27.5	3251, **3061, 3050, 3010,** 2858	Contact zone above tsunami deposit; southwest side of Nushagak Peninsula
Site 8 95CW51-4	GX-21376	4415 ± 150	−27.5	5295, **4983,** 4837	Contact zone below tsunami deposit; southwest side of Nushagak Peninsula
Site 9 95CW54-3	GX-21377	8685 ± 135	−28.1	9871, **9641, 9608, 9588,** 9490	Sample collected from beneath sand lens along coast southeast of Togiak Bay

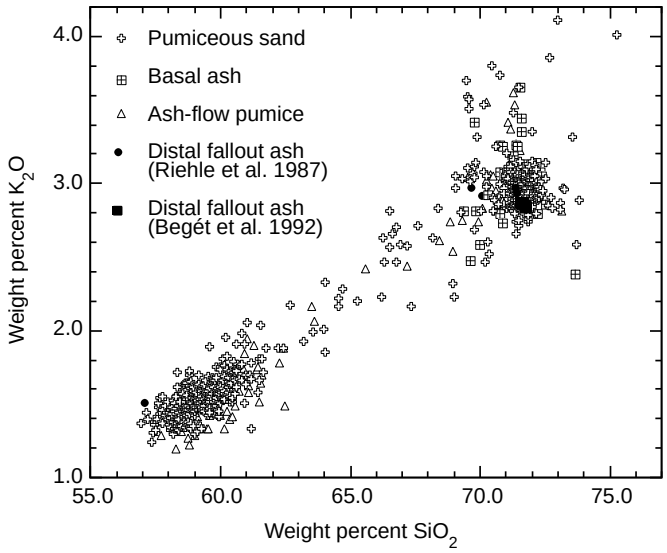

Fig. 5 Weight percent silica vs potash for samples of pumiceous sand, basal ash, ash-flow pumice, and distal Aniakchak tephra. Data from Riehle et al. (1987) and Begét et al. (1992) are average values. Data on ash-flow pumice from C Nye, Alaska Volcano Observatory

deposits (Riehle et al. 1987; Begét et al. 1992). Figure 5 shows potash vs silica for glass shards in samples of the pumiceous sand and the basal ash from four different stratigraphic sections on the Nushagak Peninsula. Data for Na_2O vs silica show a similar trend. Also shown are results for glass analyses from known Aniakchak pyroclastic-flow and fallout deposits. Although geochemical data on climactic Aniakchak fallout glass are limited, recent work by J. Riehle (pers. commun.) confirms the bimodal character of glass composition from known primary fallout. Furthermore, it has been long established that Aniakchak pyroclastic-flow deposits are compositionally zoned (Miller and Smith 1977). We are therefore confident of a compositional correlation between the pumiceous sand and the ~3500-year-old Aniakchak eruption.

Glass from basal-ash samples is more silicic than other samples of Aniakchak tephra (Fig. 5); thus, it is probably the product of a single eruptive pulse that was chemically homogeneous. This result, combined with its characteristic good sorting and mantle bedding, supports previous interpretations of this deposit (Allen 1994) as fine-grained fallout from Aniakchak.

Constituents of the pumiceous sand were identified by examining 100 loose grains from 16 samples with a binocular microscope. The average composition of the samples is 60% pumice, 22% glass shards and crystal fragments, and 18% lithic grains. Representative samples of modern beach sand ($n=6$) contain <1% pumice and glass, 37% crystal fragments, and 63% lithic grains. Dark-colored or lithic grains are not obvious in hand samples of the basal ash.

It is not possible to determine, from the composition of the sand fraction, if the original source of the pumiceous sand is fallout or pyroclastic flow/surge. Its composition spans the entire range of caldera-forming products and could be a mixture of fallout tephra, juvenile components from the ash flows, or both.

Granulometric characteristics

Median grain size and sorting for 13 samples of the pumiceous sand and four samples of modern beach sand are given in Table 2. The pumiceous sand consists of

Table 2 Particle-size statistics for pumiceous sand and beach deposits in upper Bristol Bay [Particle-size statistics from Folk 1968; IGSD = inclusive graphic standard deviation; skew = inclusive graphic skewness]

Site no.	Sample	Stratigraphic position	Cumulative percentiles					Graphic			IGSD	Skew
			5	16	50	84	95	Median	Mean	SD		
3	95CW2-A	Bulk sample	0.19	0.8	2.18	5.8	7.0	2.18	2.9	2.5	2.28	5.79
	95CW2-2	Top of massive bed	1.2	1.6	2.35	3.0	4.45	2.35	2.31	0.7	0.84	1.13
	95CW2-3	Middle of massive bed	1.2	1.75	2.8	5.64	6.4	2.8	3.39	1.94	1.76	4.68
	95CW2-4	Base of massive bed	1.2	1.61	2.51	5.15	6.17	2.51	3.09	1.77	1.64	4.28
	95CW2-6	Laminated bed	0.5	0.92	1.79	3.9	6.95	1.79	2.20	1.49	1.72	2.34
	95CW2-7	Granule-rich bed	−0.8	−0.1	0.7	1.95	6.48	0.7	0.85	1.02	1.61	−0.34
5	95CW3-1	Bulk sample	−1.75	−0.7	1.61	2.6	3.41	1.61	1.17	1.65	1.6	−3.93
	95CW3-2	Top of bed	−0.9	−0.25	0.9	3.2	6.41	0.9	1.28	1.72	1.97	1.08
	95CW3-3	Middle of bed	−0.8	0.05	1.38	5.05	7.0	1.38	2.16	2.5	2.43	5.05
	95CW3-4	Bottom of bed	−1.0	−0.4	0.85	2.15	6.15	0.85	0.86	1.28	1.72	−0.94
	95CW3-7	Beach sand	0.75	1.35	1.81	2.4	3.4	1.81	1.85	0.53	0.66	0.82
6	95CW50-1	Bulk sample	−1.3	−0.6	1.15	5.4	6.95	1.15	1.98	3.0	2.75	6.2
	95CW50-4	Beach sand	−0.9	−0.25	1.0	1.85	2.35	1.0	0.86	1.05	1.02	−1.32
8	95CW51-1	Bulk sample	−1.2	−0.7	1.2	6.1	7.4	1.2	2.2	3.4	3.0	9.0
	95CW51-5	Beach sand	0.7	1.2	1.9	2.42	2.82	1.9	1.84	0.61	0.63	0.59
7	95CW56-1	Bulk sample	−0.82	0.1	1.59	3.81	6.7	1.59	1.83	1.85	2.07	0.53
	95CW56-4	Beach sand	0.5	0.98	1.7	2.35	2.72	1.7	1.68	0.68	0.68	0.45

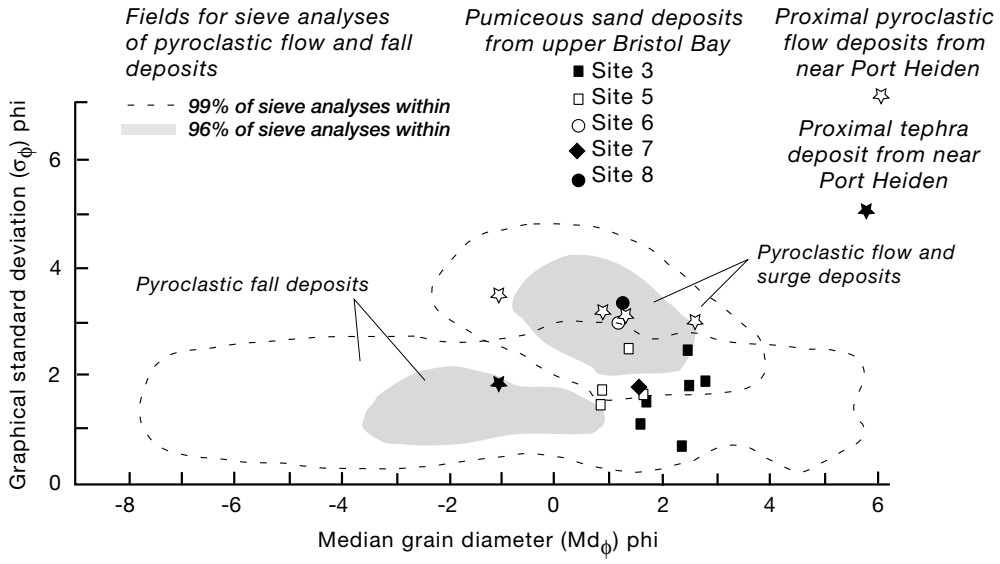

Fig. 6 Comparison of median grain diameter vs graphical standard deviation (sorting) for pumiceous sand deposits from upper Bristol Bay and pyroclastic fall and flow deposits. (Modified from Walker 1971 and Walker et al. 1980)

coarse-to-fine, moderately to very poorly sorted sand. Figure 6 shows these data superimposed on the fields for pyroclastic flow, surge, and fall deposits (Walker 1971; Walker et al. 1980); also shown are particle-size data from matrix samples of proximal pyroclastic-flow deposits and tephra (one sample) from the ~3500-years B.P. Aniakchak eruption. As a group, the pumiceous sand overlaps the fields of pyroclastic-flow and fall deposits but is generally more similar to pyroclastic-flow and surge deposits than to fall deposits. Overlap among the three fields makes it difficult to determine the mode of origin of the pumiceous sand based on grain-size data alone. Figure 7 shows the median grain diameter and sorting for the pumiceous sand compared with data for pyroclastic-flow and surge deposits from the 1883 eruption of Krakatau Volcano (Carey et al. 1996) and pyroclastic-flow deposits from the caldera-forming eruption of Aniakchak Volcano. The Krakatau deposits were transported over water and could be a possible analog for the pumiceous sand in the upper Bristol Bay area. However, the pumiceous sand is different from the Krakatau and Aniakchak pyroclastic-flow deposits (Fig. 7); it is better sorted and slightly coarser, although samples from sites 8 and 6 are similar.

The particle-size distributions for the two thickest deposits of pumiceous sand (sites 3 and 5, Fig. 1) are

Fig. 7 Median grain diameter vs inclusive graphic standard deviation (sorting) for pumiceous sand deposits from upper Bristol Bay area. Also shown are data for pyroclastic-flow and surge deposits from the 1883 Krakatau eruption, beach sand from the Bristol Bay coastline, and proximal pyroclastic-flow deposits from the ~3500-year B.P. Aniakchak eruption. Krakatau samples are 40–80 km from volcano source and were transported over water. Krakatau data from Carey et al. (1996) and Mandeville et al. (1996)

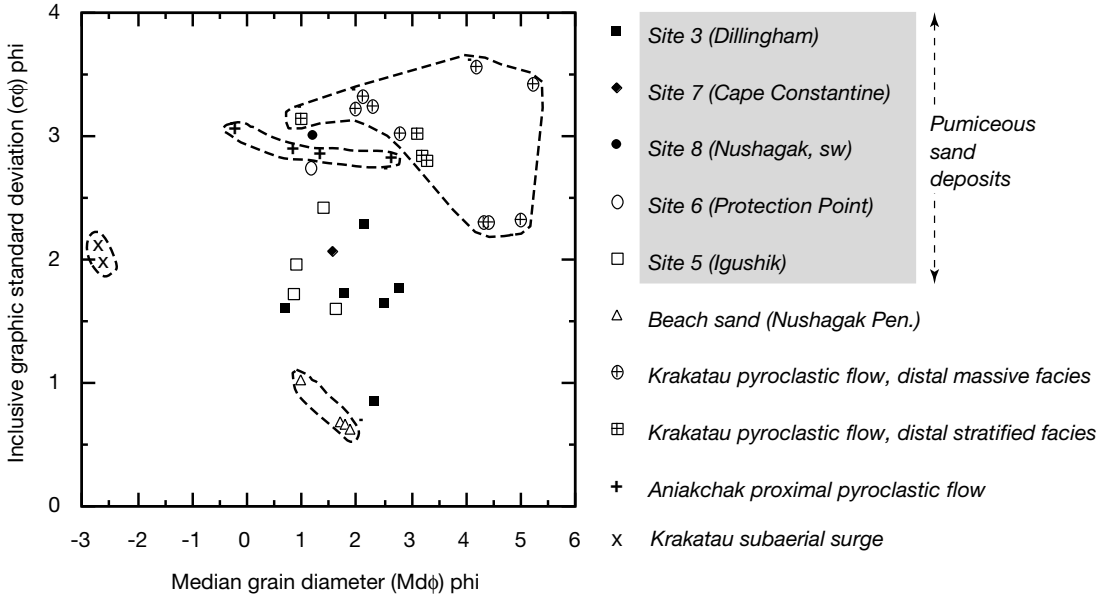

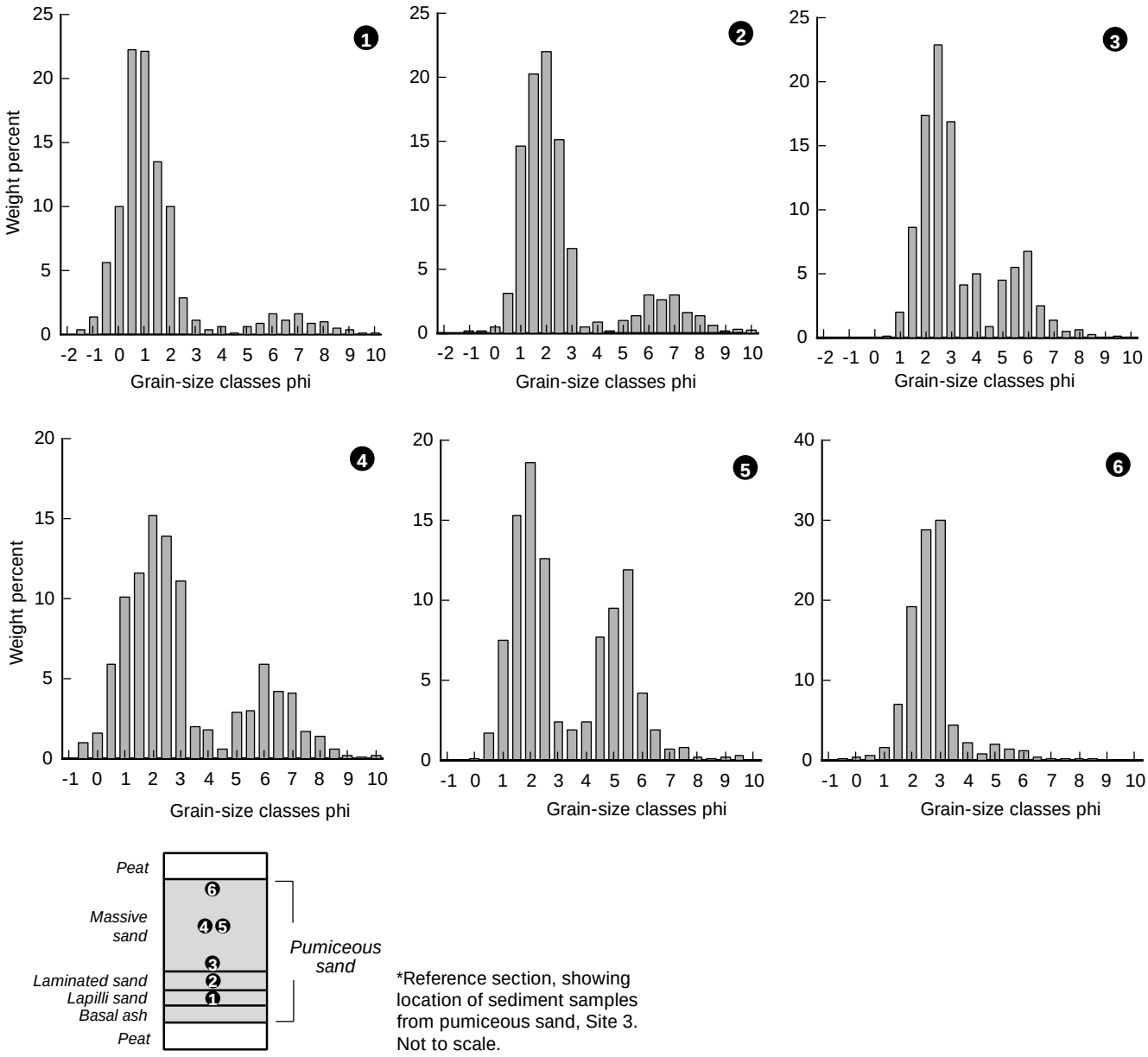

Fig. 8 Histograms of particle-size distribution for pumiceous sand deposit at site 3 (Dillingham). Reference section at bottom shows location of particle-size samples

shown in Figs. 8 and 9. At site 3 (Dillingham, Figs. 1, 8) and site 5 (Igushik, Figs. 1, 9), pumiceous sand shows crude upward fining and bimodal size distribution significantly different from that of the unimodal beach sand.

The shapes of constituent grains in the pumiceous sand were classified with a binocular microscope as angular, subangular, subrounded, or rounded, using a standard-shape chart (Powers 1953). The majority of the grains in the pumiceous sand ($n=15$) are subangular to subrounded (19% angular, 46% subangular, 35% subrounded, and $<1\%$ rounded), whereas samples of beach sand ($n=6$) are slightly more rounded (11% angular, 49% subangular, 37% subrounded, and 3% rounded).

Diatoms

Diatoms have been used successfully to identify a marine source for tsunami-deposited sand found on land (Kosugi 1988; Hemphill-Haley 1995). Thirteen samples of the pumiceous sand from seven sites (sites 1, 3, 5–8, 10, Fig. 1) were examined for diatom content by E. Hemphill-Haley of the U.S. Geological Survey. All of the samples contain abundant freshwater diatoms, and samples from sites 1, 3, 5, and 10 contain $<10\%$ brackish-marine species. Although little is known about modern diatom distribution in upper Bristol Bay, the presence of marine species in the pumiceous sand at four of the seven sites examined is good evidence of a

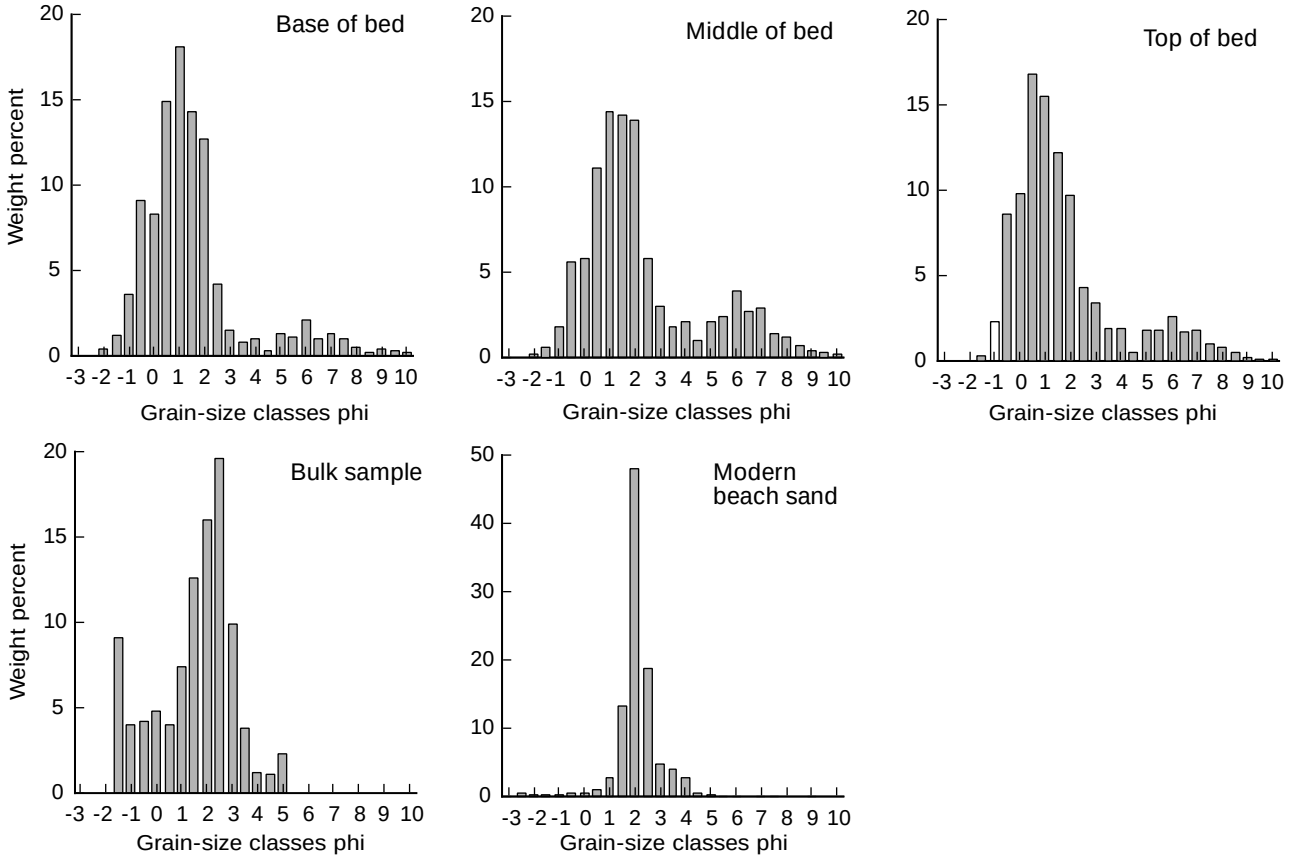

Fig. 9 Histograms of particle-size distribution for pumiceous sand deposit at Igushik (site 5). Data for Igushik beach sand also included

seaward source for the sand. The abundance of freshwater diatoms may indicate the development of a supratidal wetland soon after the pumiceous sand was deposited. Diatoms may quickly colonize freshwater wetlands and bogs (E. Hemphill-Haley, pers. commun.).

Emplacement mechanism for the pumiceous sand

The most striking characteristic of the pumiceous sand is its sudden and singular appearance as much as 15 m above present high tide within an otherwise monotonous peat sequence that began accumulating approximately 9500 years ago. Based on our observations of numerous coastal bluffs exposed almost continuously along several hundred kilometers of coastline, we conclude that the pumiceous sand represents a highly unusual process, apparently the only one of its kind in approximately 9500 years of accumulation represented by the bluff-top peat. These observations argue for a unique depositional event combining both an abundant source of pumice- and crystal-rich sand and a mechanism to carry it high above the water surface. Emplacement mechanisms we consider herein include storm surge, primary tephra fall, primary pyroclastic flow/surge, aeolian reworking, and tsunami.

Storm surge

A storm-surge origin is not consistent with the distribution of the pumiceous sand. The estimated 100-year storm surge for Bristol Bay, determined from a relation between wind speed and surge height, is 3.7 m (Wise et al. 1981). Even if this estimate were off by 100%, the height of the pumiceous sand above present high tide exceeds this elevation at several locations. Although rates of bluff erosion are unknown, modern bluff exposures represent surfaces that were probably some distance inland 3500 years ago. Thus, even larger storm waves would have been required to deposit sand at inland sites that are now coastal bluffs along Nushagak Peninsula. We thus consider it unreasonable to invoke a single storm surge of extraordinary magnitude coincident with the caldera-forming eruption of Aniakchak Volcano. Additionally, the presence of the pumiceous sand ~8 m above high tide along the Wood River bluff just north of Dillingham (site 2, Fig. 1) is inconsistent with a storm surge because this site is protected from Bristol Bay waves.

Primary tephra fallout

At most locations the pumiceous sand lacks mantle bedding and sorting characteristics typical of primary fallout (Fig. 6). The grain size of the pumiceous sand is probably too coarse to be primary fallout from the cal-

dera-forming eruption ~150 km to the south (J. Riehle, pers. commun.), although some pumice lapilli must have been deposited on the surface of Bristol Bay and rafted close to Nushagak Peninsula. Also, marine diatoms, rip-up clasts of peat, and beach sand would not be expected in primary tephra-fall deposits. We consider the discontinuous basal ash at site 3 (Fig. 2) to be part of the Aniakchak tephra-fall sequence based on its stratigraphic context, glass composition, and field appearance.

Pyroclastic flow/surge

Characteristics of the pumiceous sand that are consistent with an origin by pyroclastic flow and surge include faint bedding and lamination (sites 3 and 8, Fig. 2), widespread distribution, abundance of juvenile material, incipient rounding of pumice grains, and geochemical similarity to proximal pyroclastic-flow deposits formed during the caldera-forming eruption. As a group, samples of the pumiceous sand are slightly better sorted but coarser grained than pyroclastic-flow and surge deposits transported over water during the 1883 eruption of Krakatau (Fig. 7). The pumiceous sand shows no stratification according to clast density, as is found in some pyroclastic-flow and surge deposits, and exhibits no field evidence of high-temperature emplacement (red oxidation colors, carbonized wood, charcoal, or other burned vegetal matter; Cas and Wright 1991). Pyroclastic flows and surges from the 1883 Krakatau eruption remained hot up to approximately 65 km from their source (Carey et al. 1996). The Nushagak Peninsula is more than twice this distance from Aniakchak Volcano; thus, it seems unlikely that the pumiceous sand originated by pyroclastic flow or surge.

Aeolian

In most places the pumiceous sand is massive and lacks internal structures indicative of transport by wind, such as well-defined high-angle cross bedding or subhorizontal bedding. Furthermore, fragile grains of pumice and glass show minimal evidence of rounding, and the amount of detrital material in the deposit is low. Nearby beaches could have been a source of sand for aeolian transport, but the ubiquitous lack of other sand layers in the peat cap around the Nushagak Peninsula area would imply a single burst of wind coincident with the caldera-forming eruption of Aniakchak Volcano. Although air blasts do occur during some eruptions, it is unlikely that such a blast could travel the approximately 150 km to the Nushagak Peninsula and maintain sufficient velocity to entrain and transport the pumiceous sand from the beach up and over >15-m-high coastal bluffs.

Tsunami

Our preferred explanation of the pumiceous sand is that it was deposited by a tsunami generated by the rapid flow of pyroclastic material into the sea during the caldera-forming eruption of Aniakchak Volcano ~3500 years B.P. (Fig. 10). The distribution of the pumiceous sand along the shoreline, presence of marine diatoms and rip-up clasts of peat, abrupt lower contact, partial rounding of pumice grains, and stratigraphic uniqueness within a continuous, 9500-year sequence of peat are all consistent with an origin by a locally generated tsunami. The stratigraphic context of the pumiceous sand (i.e., an exotic sand bed in peat or tidal deposits) is similar to that of other tsunami deposits in Scotland (Long et al. 1989), British Columbia (Clague and Bobrowsky 1994; Benson et al. 1997), Washington (Atwater and Hemphill-Haley 1997), and Japan (Minoura et al. 1994; Nishimura and Miyaji 1995).

Mechanism of tsunami generation

How could tsunami be generated in Bristol Bay? Lea (1989) suggested an earthquake origin for the tsunami, coincident with the formation of Aniakchak caldera. For reasons discussed later, we favor the sudden ingress of voluminous, fast-moving pyroclastic flows along a 55-km segment of Bristol Bay as the mechanism for tsunami generation. A sediment source would have been provided by the accumulation, flotation, and partial suspension of pumiceous fallout tephra from the climactic Aniakchak eruption, as well as by local beach sand along the upper Bristol Bay coastline. Rafting of pumiceous fallout tephra against the northern coastline of Bristol Bay is likely to have occurred, especially if prevailing late Holocene winds and longshore currents were similar to those that exist presently.

A syneruptive (or nearly so) tectonic earthquake of sufficient magnitude to produce tsunami of the size required to deposit the pumiceous sand is improbable but cannot be ruled out. Firstly, the earthquake would have had to occur fortuitously in a time indistinguishable from that of the caldera-forming event, approximately 100 years given uncertainties in radiocarbon dating. Secondly, there are no young high-angle faults on arc-parallel structures beneath Bristol Bay (D. Scholl, pers. commun.), so that the required sea-floor displacement during a shallow earthquake apparently could not occur. Finally, based on historical records, a large Aleutian megathrust, back arc, or distant tectonic earthquake is unlikely to generate a wave of significant size in Bristol Bay. Since 1737 there have been a few reports of tsunami in Bristol Bay related to earthquakes, but none was associated with significant run up or coastal damage (Lander 1996).

Another source of strong seismicity is that related to the formation of large calderas (Newhall and Dzurisin

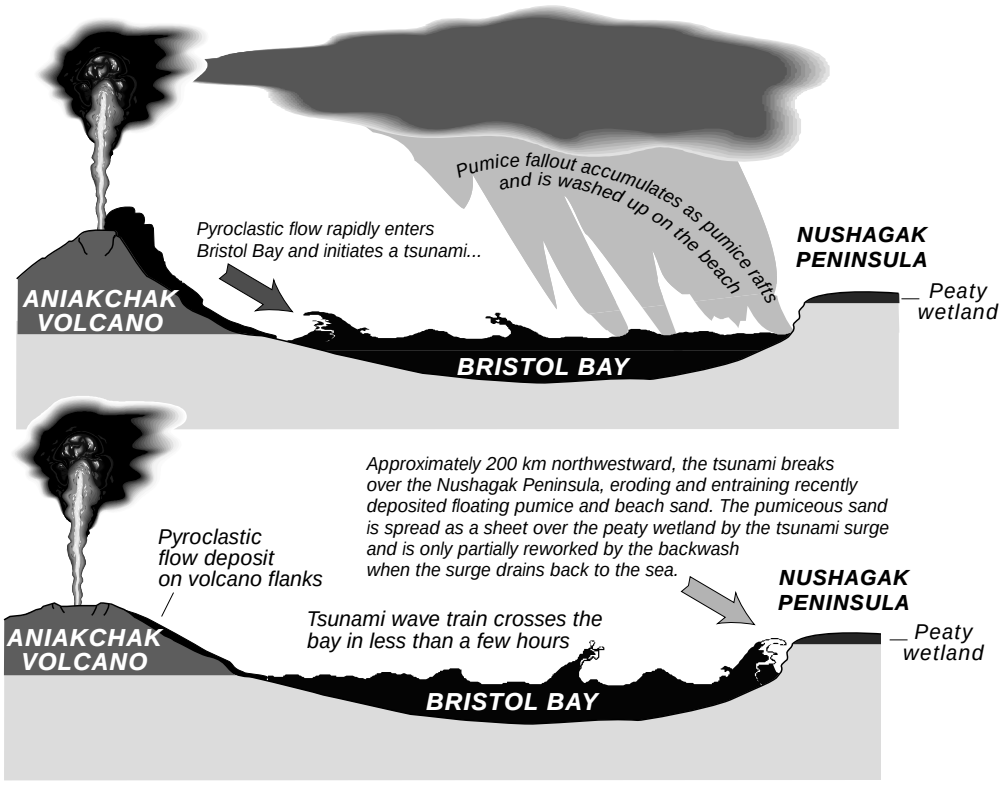

Fig. 10 Tsunami initiation by pyroclastic flow at Aniakchak Volcano

1988). The eruption of Novarupta and the caldera collapse of Mount Katmai in 1912 produced 14 earthquakes of Ms 6.0 or greater, including an Ms 7.0 earthquake (Hildreth 1991; Abe 1992). However, these earthquakes represent shallow and largely vertical crustal displacements within and below the volcanic edifice. For Aniakchak, the epicenter(s) of caldera-forming earthquakes would be 30–60 km from the Bristol Bay coastline and therefore too far inland to significantly displace the seafloor and generate a tsunami.

Our favored mechanism for tsunami generation is the rapid emplacement of pyroclastic flows into the southern part of Bristol Bay (Figs. 1, 10). Rapid, syneruptive emplacement of pyroclastic flows into the sea has produced significant tsunami during large explosive eruptions in historical times, most notably at Krakatau in 1883 (Self and Rampino 1981; Carey et al. 1996) and Tambora in 1815 (Self et al. 1984; Stothers 1984). A damaging tsunami also was produced by pyroclastic flows entering the sea during the 1902 eruption of Mount Pelee on the island of Martinique (LaCroix 1904).

The September to October 1994 eruption at Rabaul Caldera in Papua, New Guinea, provides a possible analog for the deposition of the pumiceous sand in upper Bristol Bay. During the first 2 days of plinian eruptive activity on 19–20 September, pyroclastic flows cascading into the sea caused damaging tsunami with local runup to 5–6 m (B. Talai, pers. commun.). Deposits from these tsunami on beaches are highly variable in thickness and consist of poorly sorted, coarse pumice carried as much as 100 m inland (Blong 1995). The pumice was originally deposited by fallout on the surface of Simpson Harbor and formed concentrated rafts of floating pumice (Fig. 11).

An additional mechanism for generating tsunami in Bristol Bay is submarine slumping of unconsolidated pyroclastic-flow deposits that came to rest offshore. Slumping of newly emplaced, submarine pyroclastic-flow deposits to form turbidites was described at Mount Pelee; however, no tsunami was recorded that can be tied to this process (Carey and Sigurdsson 1978). Other tsunami associated with the 18 September 1994, eruption at Rabaul Caldera may have been caused by seismically induced slumping of unconsolidated sediments that predated the eruption (B. Talai, pers. commun. 1995).

Tsunami generation by pyroclastic flow

Pyroclastic flows from the climactic eruption of Aniakchak Volcano could have initiated a tsunami in the following manner. The possible types of interaction of hot pyroclastic flows and cold ocean water depend on the density and angle of incidence of the flow (Cas and Wright 1991). Ash-flow tuff in sea cliffs along Bristol Bay northeast of Port Heiden, 30–60 km from the caldera (Fig. 1), consists of a single $\geq$15-m-thick, massive, matrix-supported bed composed of low-density pumice and scoria and minor amounts of lithic material (Miller and Smith 1977). The pyroclastic-flow deposit mantles a low-relief coastal plain. The flows reached southern

Fig. 11 Simpson Harbor, New Britain Island, Papua New Guinea, June 1994. *Dark material* at head of harbor is floating raft of pumice produced by the 1994 eruption of Rabaul Volcano. Small tsunami entrained some of this pumice and formed thin sheets of pumiceous sand along the coastline. A similar process likely occurred to form the pumiceous sand deposit during the ~3500-year B.P. eruption of Aniakchak Volcano. (Courtesy of N. Lauer)

Bristol Bay at a low angle and were probably decelerating, deflating, and beginning to deposit pyroclastic debris as they entered the water. Although the geometry of the flow front is unknown, the areal extent of the ash-flow sheet suggests a width of approximately 55 km and a thickness of at least 15 m (Miller and Smith 1977). Because we do not know how far the flow extended into the ocean, we cannot estimate the volume of seawater that the pyroclastic flow displaced.

The most efficient way for a pyroclastic flow to generate a tsunami is to displace water across a broad front almost instantaneously. Assuming that the density of the pyroclastic flow is greater than that of seawater, the process is analogous to a piston-like impulse that generates a free-surface gravity wave. Beyond the point of impact of the pyroclastic flow with the sea, the wave could behave like a shallow-water solitary wave or a surge wave or bore.

The propagation speed *(c)* of solitary waves and bores is:

$$c = \sqrt{g\,d} \tag{1}$$

where g is gravitational acceleration (9.8 m/s^2) and d is water depth. The average water depth of upper Bristol Bay is ~30 m; thus, the tsunami would advance at approximately 17 m/s (assuming uniform water depth) and take approximately 2 h to reach Nushagak Peninsula. As the wave approaches the Bristol Bay coastline and the water depth decreases, wave energy is dissipated through interaction of the wave and the sea bottom. The wave will entrain sediment when the bed stress exceeds the immersed weight of the sediment grains.

Because of radial spreading, the tsunami wave height will decrease somewhat during propagation across Bristol Bay. If the tsunami wave behaves like a solitary wave, the maximum stable wave height will be approximately 0.78 times the water depth (Komar 1976). Since the water depth just off Nushagak Peninsula is approximately 10 m, the maximum stable wave height is ~7.8 m and the speed of the wave is approximately 10 m/s.

The threshold stress (τ_c) required for entrainment of sand from a uniform bed is 0.56 g/cm s^2 according to the relation (Komar 1989):

$$\tau_c = 0.00515 (\quad \mathrm{v}_f) g\,D$$

where ρ_s is the grain density (2.65 gm/cm^3), ρ_f is the fluid density (1.146 gm/cm^3), g is gravitational acceleration, D is grain diameter, and tan Φ is the tangent of the grain pivot angle (ca. 0.6 for grains of uniform size). The critical shear velocity (U_c) required to entrain medium-to-fine sand from a bed of uniform grains is approximately 0.7 cm/s according to the relation (Martinez and Harbaugh 1993):

$$U_c = \left(\frac{\rho_f}{}\right)^{\frac{1}{2}} \tag{3}$$

If the speed of the tsunami wave were approximately 10 m/s, as for a wave ~7.8 m high, it would have been capable of entraining sand-sized particles from the nearshore environment (including beach sand and pumice grains) to form the pumiceous sand found around Nushagak Peninsula and upper Bristol Bay.

Conclusion

An unusual pumiceous sand sheet within Holocene peat deposits along the coastline of upper Bristol Bay, Alaska, was probably deposited by a tsunami during the ~3500-year B.P. eruption of Aniakchak Volcano. The tsunami was probably caused by the rapid ingress of a large volume pyroclastic flow into southern Bristol Bay. Distal pumice-rich fallout lapilli and local beach sand were the sources of the tsunami sand sheet. The tsunami wave, which could have been as high as 7.8 m just off Nushagak Peninsula, swept up and over coastal bluffs and inundated a peat-covered lowland that pres-

ently is ≤ 15 m above sea level. The pumiceous sand was deposited over the coastal fringe of the lowland and later buried by renewed peat accumulation.

Eruptive products from the caldera-forming eruption of Aniakchak Volcano exceed 50 km^3 in volume (Miller and Smith 1987), and as much as 75% of this volume is pyroclastic-flow deposits. Similar-sized caldera-forming eruptions of Holocene age occurred at three other volcanic centers on the Alaska Peninsula and eastern Aleutian Islands (Okmok, Fisher, and Veniaminof; Miller and Smith 1987), and slightly smaller eruptions (10–50 km^3 bulk volume of eruptive material) took place at two other volcanic centers (Kaguyak and Black Peak; Miller and Smith 1987). Like Aniakchak, these eruptions generated extensive sheets of pyroclastic debris, some of which are well exposed in modern sea bluffs along the Bering Sea coastline. At least some of these large-volume caldera-forming eruptions on the Alaska Peninsula and eastern Aleutian Islands were capable of initiating tsunami in the manner we propose for Aniakchak Volcano, although tsunami deposits related to these large eruptions have yet to be located and studied.

Acknowledgements We thank P. Lea and D. Kaufman, who stimulated our interest in this study and shared unpublished field data. Discussions with G. McGimsey, T. Miller, J. Riehle, A. Roach, E. Geist, and D. Scholl helped clarify several important aspects of our paper. E. Hemphill-Haley provided diatom analyses, M. Harbin helped obtain geochemical data, R. Forkner assisted with point counting, and B. Talai provided information about the 1994 Rabaul eruption. Excellent reviews by C. Gardner, A. Nelson, J. Begét, A. Moore, and G. Fryer helped improve the manuscript.

References

Abe K (1992) Seismicity of the great eruption of Mount Katmai, Alaska, in 1912. Bull Seismol Soc Am 82 (1): 175–191

Allen BM (1994) Holocene tephra and tsunami deposits along western Nushagak Bay, southwestern Alaska. Geol Soc Am, Northeastern Section, Abstracts with Programs 26:2

Atwater BF, Hemphill-Haley E (1997) Recurrence intervals for great earthquakes of the past 3500 years at northeastern Willapa Bay, Washington. US Geol Surv Prof Pap 1576

Begét JE, Kienle J (1992) Cyclic formation of debris avalanches at Mount St. Augustine Volcano, Alaska. Nature 356:701–704

Begét J, Mason O, Anderson P (1992) Age, extent, and climatic significance of the c. 3400 BP Aniakchak tephra, western Alaska, USA. The Holocene 2 (1): 51–56

Benson BE, Grimm KA, Clague JJ (1997) Tsunami deposits beneath tidal marshes on northwestern Vancouver Island, British Columbia. Quaternary Res 48:192–204

Blong R (1995) The Rabaul eruption 1994, destruction of a town. Natural Hazards Research Centre, Sydney, Australia

Carey SN, Sigurdsson H (1978) Deep-sea evidence for distribution of tephra from the mixed magma eruption of the Soufriere on St. Vincent 1902: ash turbidites and air fall. Geology 6:271–274

Carey SN, Sigurdsson H, Mandeville C, Bronto S (1996) Pyroclastic surges and flows over water: an example from the 1883 Krakatau eruption. Bull Volcanol 57:493–511

Cas RAF, Wright JV (1991) Subaqueous pyroclastic flows and ignimbrites: an assessment. Bull Volcanol 53:357–380

Clague JJ, Bobrowsky PT (1994) Tsunami deposits beneath tidal marshes on Vancouver Island, British Columbia. Geol Soc Am Bull 106:1293–1303

Folk RL (1968) Petrology of sedimentary rocks. Hemphill, Austin, Texas

Hemphill-Haley E (1995) Diatom evidence for earthquake-induced subsidence and tsunami 300 years ago in southern coastal Washington. Geol Soc Am Bull 107:367–378

Hildreth W (1991) The timing of caldera collapse at Mount Katmai in response to magma withdrawal toward Novarupta. Geophys Res Lett 18 (8): 1541–1544

Kienle J, Kowalik Z, Murty TS (1987) Tsunamis generated by eruptions from Mount St. Augustine Volcano, Alaska. Science 236:1442–1447

Komar PD (1976) Beach processes and sedimentation. Prentice-Hall, Englewood Cliffs, New Jersey

Komar PD (1989) Physical processes of waves and currents and the formation of marine placers. CRC Critical Reviews in Aquatic Sciences, Oregon Sea Grant, Oregon State University 1:393–423

Kosugi M (1988) Classification of living diatom assemblages as the indicator of environments, and its application to reconstruction of paleoenvironments. Quaternary Res (Japan) 27:1–20

LaCroix A (1904) LaMontagne Pelee et ses eruptions. Masson, Paris, pp 1–653

Lander JF (1996) Tsunamis affecting Alaska 1737–1996. National Geophysical Data Center, Geophysical Research Documentation 31:1–195

Latter JH (1981) Tsunamis of volcanic origin: summary of causes, with particular reference to Krakatoa, 1883. Bull Volcanol 44 (3): 467–490

Lea PD (1989) Holocene tsunami deposits in coastal peatlands, northeastern Bristol Bay, SW Alaska. Geol Soc Am Abstracts with Programs 21 (6): A344

Lea PD (1990) Pleistocene periglacial eolian deposits in southwestern Alaska: sedimentary facies and depositional processes. J Sediment Petrol 60:582–591

Lea PD, Elias SA, Short SK (1991) Stratigraphy and paleoenvironments of Pleistocene nonglacial deposits in the southern Nushagak lowland, southwestern Alaska, USA. Arctic Alpine Res 23:375–391

Long D, Smith DE, Dawson AG (1989) A Holocene tsunami deposit in eastern Scotland. J Quaternary Sci 4:61–66

Mandeville CW, Carey SN, Sigurdsson H (1996) Sedimentology of the Krakatau 1883 submarine pyroclastic deposits. Bull Volcanol 57:512–529

Martinez PA, Harbaugh JH (1993) Simulating nearshore environments. Pergamon Press, Oxford

Miller TP, Smith RL (1977) Spectacular mobility of ash flows around Aniakchak and Fisher Calderas, Alaska. Geology 5:434–438

Miller TP, Smith RL (1987) Late-Quaternary caldera-forming eruptions in the eastern Aleutian Arc, Alaska. Geology 15:173–176

Minoura K, Nakaya S, Uchida M (1994) Tsunami deposits in a lacustrine sequence of the Sanriku coast, northeast Japan. Sediment Geol 89:25–31

Neal CA, McGimsey RG, Waythomas CF, Miller TP, Nye CJ (1995) The last 3400 years at Aniakchak Caldera, Alaska. Geol Soc Am Abstracts with Programs 27 (5): 66

Newhall CG, Dzurisin D (1988) Historical unrest at large calderas of the world. US Geol Surv Bull 1855

Nishimura Y, Miyaji N (1995) Tsunami deposits from the 1993 southwest Hokkaido earthquake and the 1640 Hokkaido Komagatake eruption, northern Japan. Pure Appl Geophys 144:719–733

Nomanbhoy N, Satake K (1995) Generation mechanism of tsunamis from the 1883 Krakatau eruption. Geophys Res Lett 22:509–512

Powers MC (1953) A new roundness scale for sedimentary particles. J Sediment Petrol 23:117–119

Prins JE (1958) Characteristics of waves generated by a local disturbance. EOS Trans Am Geophys Union 39:865
Riehle J, Meyer C, Ager T, Kaufman D, Ackerman R (1987) The Aniakchak tephra deposit, a late Holocene marker horizon in western Alaska. US Geol Surv Circ 998:9–22
Self S, Rampino MR (1981) The 1883 eruption of Krakatau. Nature 294:699–704
Self S, Rampino MR, Newton MS, Wolff JA (1984) Volcanological study of the great Tambora eruption of 1815. Geology 12:659–663
Siebert L, Begét JE, Glicken H (1995) The 1883 and late-prehistoric eruptions of Augustine Volcano, Alaska. J Volcanol Geotherm Res 66:367–395
Stothers RB (1984) The great Tambora eruption in 1815 and its aftermath. Science 224:1191–1198
Stuiver M, Reimer P (1993) Extended ^{14}C data base and revised CALIB 3.0 ^{14}C age calibration program. Radiocarbon 35:215–230
Troshina EN (1996) Tsunami waves generated by Mt. St. Augustine Volcano, Alaska. M.Sc. thesis, University of Alaska, Fairbanks, 84 pp
Walker GPL (1971) Grain size characteristics of pyroclastic deposits. J Geol 70:409-428
Walker GPL, Wilson CJN, Froggatt L (1980) Fines-depleted ignimbrite in New Zealand: the product of a turbulent pyroclastic flow. Geology 8:245–249
Waythomas CF (1997) Debris-avalanche-initiated tsunamis at Augustine Volcano, Alaska, reexamined. Geol Soc Am Abstracts with Programs 29:73
Waythomas CF, Dorava JM, Miller TP, McGimsey RG, Neal CA (1998) Preliminary volcano hazards assessment for Redoubt Volcano, Alaska. US Geol Surv Open-File Rep 97–857:1–40
Waythomas CF, Neal CA, McGimsey RG, Dorava JM, Lemke KA, Vanderpool A (1995) Volcanigenic tsunami from Alaskan volcanoes: geologic evidence from Bristol Bay and Cook Inlet, Alaska. EOS Trans Am Geophys Union 76 (46): F291
Wise JL, Comiskey AL, Becker R Jr (1981) Storm surge climatology and forecasting in Alaska. Arctic Environmental Information and Data Center, Anchorage, Alaska